AD NUMBER

AD876458

LIMITATION CHANGES

TO:

Approved for public release; distribution is unlimited.

FROM:

**Distribution authorized to U.S. Gov't. agencies and their contractors;
Administrative/Operational Use; NOV 1970. Other requests shall be referred to Arnold Engineering and Development Center, Arnold AFB, TN.**

AUTHORITY

AEDC ltr 9 Jul 1974

AEDC-TR-70-205

Copy

NEW VELOCITY MEASURING TECHNIQUE USING DUAL-SCATTER LASER DOPPLER SHIFT

D. B. Brayton and W. H. Goethert

ARO, Inc.

November 1970

ARNOLD ENGINEERING DEVELOPMENT CENTER
AIR FORCE SYSTEMS COMMAND
ARNOLD AIR FORCE STATION, TENNESSEE

NOTICES

When U. S. Government drawings specifications, or other data are used for any purpose other than a definitely related Government procurement operation, the Government thereby incurs no responsibility nor any obligation whatsoever, and the fact that the Government may have formulated, furnished, or in any way supplied the said drawings, specifications, or other data, is not to be regarded by implication or otherwise, or in any manner licensing the holder or any other person or corporation, or conveying any rights or permission to manufacture, use, or sell any patented invention that may in any way be related thereto.

Qualified users may obtain copies of this report from the Defense Documentation Center.

References to named commercial products in this report are not to be considered in any sense as an endorsement of the product by the United States Air Force or the Government.

NEW VELOCITY MEASURING TECHNIQUE USING DUAL-SCATTER LASER DOPPLER SHIFT

D. B. Brayton and W. H. Goethert
ARO, Inc.

FOREWORD

The work reported herein was sponsored by Headquarters, Arnold Engineering Development Center (AEDC), Air Force Systems Command (AFSC), under Program Element 65701F, Project 4344, Task 32.

The results of this research were obtained by ARO, Inc. (a subsidiary of Sverdrup & Parcel and Associates, Inc.), contract operator of AEDC, AFSC, Arnold Air Force Station, Tennessee, under Contract F40600-71-C-0002. The research was performed from July 1969 to July 1970 under ARO Project No. BC5019 and the manuscript was submitted for publication on June 26, 1970.

This technical report has been reviewed and is approved.

David G. Francis
1Lt, USAF
Research and Development Division
Directorate of Technology

Harry L. Maynard
Colonel, USAF
Director of Technology

ABSTRACT

Conventional laser Doppler velocimeters (LDV) detect velocity by heterodyning scattered, Doppler shifted radiation with unscattered, reference radiation. A new dual-scatter LDV technique is described which simultaneously illuminates a moving scatterer from two different directions and heterodynes the two superimposed radiations simultaneously scattered in a common direction. Significant advantages are derived from the fact that the Doppler difference frequency thus obtained is independent of the scattered direction, permitting unusually large quantities of scattering radiation to be collected without adversely affecting the signal frequency dispersion; these advantages include enhanced signal-to-noise performance and a capability to measure fluid flows with unusually high velocity and/ or low seed density. System performance, experimental verifications, and typical system designs are presented.

CONTENTS

APPENDIX
Illustrations

Figure

SECTION I
INTRODUCTION

A laser Doppler velocimeter (LDV) is an instrument that employs optical heterodyne techniques to measure the velocity of moving solids, liquids, or gases without perturbing the velocity being detected. Most of the numerous LDVs developed to date (Refs. 1 and 2) are of the reference beam type and detect velocity by heterodyning Doppler shifted scatter or reflected laser radiation with unscattered, reference radiation. Such devices can be used to accurately measure rapidly fluctuating velocities ranging from less than 1 cm/sec to thousands of feet per second.

This report discusses a newly developed crossed-laser-beams, dual-scatter LDV technique which was conceived and has been under development for more than two years at AEDC. Similar or related dual-scatter techniques are concurrently being developed elsewhere (Refs. 3 through 6). Dual scatter implies that a reference beam is not employed, but that two different scattered radiations are heterodyned to detect velocity. There exists a single illuminating beam, output aligned, dual-scatter, LDV technique (Refs. 1 and 3) which, in almost all respects, performs similarly (Ref. 1) to the dual-scatter LDV which is discussed here.

The basic principles of the dual-scatter LDV will be described by a fringe formation approach which is easily understood and readily provides a basic understanding of the system performance parameters. There exists an alternate approach (Ref. 1) which involves calculation of the Doppler frequency shifts of two radiations simultaneously scattered from a common source, in a common direction, and from two different illuminating beams; the Doppler difference frequency can then be shown to be constant and independent of the viewing direction. However, with the latter approach, one cannot as readily describe how various parameters affect the overall system performance.

The objectives of this report are (1) to present an easily understandable explanation of the crossed-laser-beams, dual-scatter LDV in such a way that (2) the performance characteristics of this system evolve from the discussion, (3) to provide experimental evidence that the predicted performance characteristics are correct, and (4) to discuss the performance relative to reference beam LDV systems. Although the dual-scatter LDV technique presented has been successfully

employed in a number of different applications (Ref. 1), these are not discussed here because they are beyond the scope of this report.

SECTION II
FRINGE FORMATION AND VELOCITY COMPONENT DETECTION

The dual-scatter LDV optical system is shown in Fig. 1 (Appendix). Two quasi-monochromatic plane polarized, collimated, TEM_{00} (Gaussian) laser beams of approximately 1-mm diameter are caused to focus to a common point (0, 0, 0) in the test region by a set of self-aligning illuminating optics similar to those previously used with a crossed-beam, reference beam velocimeter (Ref. 7). These optics consist of two 1-in. -thick, plane parallel glass blocks and a positive collimating lens. The plane parallel blocks, when properly coated, cause the collimated beam exiting from the laser to split into two equal intensity collimated output beams which propagate parallel to one another. The second block serves to increase the distance separating the two beams and to equalize optical path lengths. (To produce optical interference effects, equal optical path lengths may or may not be required depending on the laser employed.) A positive lens will focus all parallel input rays to a common point (0, 0, 0) and will maintain equal optical path lengths. The two beams thus converge and focus to (0, 0, 0) such that the two radiations are spatially and temporally coherent near (0, 0, 0). Figure 1b is a multiple exposure that shows the self-aligning illuminating optics illuminated by a laser.

Each laser beam will focus to a long, narrow, pencil-shaped diffraction region of Gaussian intensity distribution which contains essentially planar phase fronts (Ref. 8), as indicated in Fig. 2a. Because the two radiations are mutually coherent and identically polarized, they will interfere constructively and destructively to establish a set of closely spaced, planar interference fringes in the beam crossover region. Such fringes, shown in Fig. 2b, consist of plane parallel regions of maximum and minimum illuminating intensity caused by constructive and destructive interference, respectively, of the two radiations.

Figure 2b indicates the means by which these bright and dark regions or interference fringes are formed. The edge view of the wave crests of each illuminating beam is shown as lines perpendicular to the beam centerline, such that adjacent crests are separated by the wavelength, λ. Planar wave crests from one beam, traveling at the

speed of light and parallel to the beam centerline, remain in phase with and reinforce wave crests of the other beam along planes = y constant. Such planes of peak illumination or bright fringes are indicated as lines orthogonal to the y axis of Fig. 2b. At intermediate points between the bright fringes, the two waves remain out of phase as they propagate and cancel one another (a positive wave crest being cancelled by a negative crest or valley), thus forming planes of minimum illumination or dark fringes. For the fringe formation discussion to be entirely correct, such that total constructive and destructive interference effects (bright and dark regions) will result, it must be assumed that the two radiations are plane polarized in a common direction such that either the electric or the magnetic field vectors of the two radiations are parallel in the crossover region and parallel to the x axis of Fig. 2b. Such a condition is achieved by illuminating the blocks of Fig. 1a with a plane polarized laser beam with its polarization plane oriented either parallel or perpendicular to the plane of incidence. The beam crossover region thus consists of an alternating series of plane parallel bright and dark regions or interference fringes.

An inspection of Fig. 2b will reveal that any two adjacent bright fringes are separated by a distance

$$\Delta y = \frac{\lambda}{2 \sin (\theta/2)} \tag{1}$$

where λ is the wavelength and θ is the angle between the illuminating beams.

Operation of the velocimeter is typified by its use to detect the velocity of a moving semitransparent medium (e.g., smoke seeded air flow). As a moving scatter center passes through the focal region, near (0, 0, 0), it will intercept the previously discussed interference fringes, and the illumination level it experiences will alternate from maximum to minimum to maximum to minimum, repetitively. Assume that an electro-optical detection scheme is now established such as the collecting lens-pinhole-photomultiplier tube combination of Fig. 1a which collects light radiated from a scatterer near (0, 0, 0) and displays an electrical signal (e.g., photomultiplier tube current) with an amplitude that varies in proportion to the amount of light collected. As a scatter center passes through the probe region near (0, 0, 0) because of the presence of the fringes, it will alternately scatter and then not scatter, repetitively, light into the detector and will generate an alternating, fluctuating, detector current with a fluctuation frequency that will be proportional to the rate at which the particle intercepts the

fringes, that is, proportional to the velocity component of the particle orthogonal to the fringes v_y. Equation (1) implies that v_y will be given by

$$v_y = \frac{\lambda}{2 \sin (\theta/2)} f_D \qquad (2)$$

where f_D is the frequency of the detected current.

Thus, a simple technique to detect a particular velocity component of a moving semitransparent medium has been established. The technique senses only one component of velocity: namely, that component which is oriented normal to the interference fringes.

Note that the detected signal frequency, f_D, is independent of the direction in which scattered light is collected and detected. A scatterer located on a dark fringe, for example, would not scatter light, regardless of the viewing direction. Thus, the signal strength can be increased by collecting larger quantities of scattered light by increasing the collection solid angle, and such increased collection will not alter the characteristic frequency of the received signal. It is this fact which for some applications, particularly high velocity and/or low seed density, render the dual-scatter technique potentially more sensitive and thus superior to reference beam heterodyning techniques. When reference beam heterodyning is employed, the detection solid angle of scattered radiation must be limited to limit frequency broadening effects (Refs. 1, 2, and 7).

Figure 3 contains photographs of oscilloscope displays of real-time signal currents generated when single particle atmospheric impurity constituents, such as dust normally present in a laboratory, passed through the probe volume. The particle velocities were generated by placing the velocimeter approximately 3 ft away from an exhaust duct with the probe volume fringes oriented approximately normal to the local velocity. The variations in the data of Fig. 3 are caused by the various trajectories that a scatter center can follow in passing through the probe volume and by changes in the beam intensity ratio and the beam separation distance D (Fig. 1a).

When a scatter center passes approximately through the center of the probe volume, i. e., along the y axis of Fig. 2b, the intensities of the two illuminating beams are identical and the particle intercepts fringes of infinite contrast ratio. The intensity of an illuminating beam is obtained in Fig. 2b by projecting, from the point of interest, a line parallel to the beam centerline to the Gaussian radial intensity distribution curve for that beam. Thus, for y-axis particle trajectories,

one would expect current versus time displays with current excursions returning to zero amplitude (corresponding to dark fringe particle positions) and with peak current excursions (corresponding to bright fringe particle positions) varying in a Gaussian fashion similar to the variation of the individual beam intensities. Such trajectories are evident in the selected random data of Fig. 3a.

On the displays of Fig. 3b, particles did not pass very close to the y axis (Fig. 2b) and thus intercepted fringes of finite (noninfinite) contrast ratio because of the unequal values of the beam intensities experienced. For a particle trajectory of path a-a′ of Fig. 2b, a d-c level increase would be expected with very little signal information because of the dominance of beam 1, beam 2 being very weak at the center of beam 1. Then an increase would be expected in a-c signal with current and intensity excursions returning approximately to zero amplitude (beam 2 becoming more dominant and of intensity equal to that of beam 1). Finally, when centered on beam 2, a situation similar to that when centered on beam 1 would be expected. Such current versus time displays are evident in the selected random data of Fig. 3b.

SECTION III
PROBE VOLUME

The system will have excellent spatial resolution as each laser beam focuses to a Gaussian spot of ($1/e^2$ intensity) diameter $2b_o$ (see Figs. 1 and 2) given by Ref. (8)

$$2b_o = \frac{4}{\pi}\frac{f_L}{2b}\lambda = \frac{4}{\pi}F\lambda \tag{3}$$

where $2b_o$ is typically 0.06 mm assuming the "f number" $F = f_L/(2b) = 100$, and $\lambda = 5 \times 10^{-4}$ mm.

The variables of Eq. (3) are shown in Figs. 1 and 2; f_L is the focal length of the beam focusing lens, and 2b is the ($1/e^2$ intensity) diameter of the input laser beam. The (x, y, z) dimensions of the beam crossover, or common overlap, region are, by inspection of Fig. 2b

$$\begin{aligned} \Delta x(1/e^2) &= 2b_o \\ \Delta y(1/e^2) &= 2b_o/\cos(\theta/2) \\ \Delta z(1/e^2) &= 2b_o/\sin(\theta/2) \end{aligned} \tag{4}$$

Signal contributions of significant amplitude are generated by scatter centers located within the volume of the beam overlap region which has these maximum dimensions. For a $1/e^2$ focal spot diameter (Eq. (3)) of $2b_o = 0.06$ mm and $\theta = 11$ deg, these dimensions are $\Delta x \approx \Delta y \approx 0.06$ mm and $\Delta z \approx 0.60$ mm. Outside of this region at least one of the beams is of much reduced intensity and contributes very little to the formation of interference fringes.

A more qualitative analysis will reveal that when a scatter center is located on the ellipsoid

$$x^2 + y^2 \cos^2(\theta/2) + z^2 \sin^2(\theta/2) = b_o^2 \tag{5}$$

the signal current excursions will be of amplitude $1/e^2$ relative to those signal current excursions which would exist if the same scatterer were located near the geometrical center of the probe volume (0, 0, 0). Similarly when on the ellipsoid

$$x^2 + y^2 \cos^2(\theta/2) + z^2 \sin^2(\theta/2) = b_o^2/2 \tag{6}$$

the signal current excursions will be of 1/e relative amplitude. These ellipsoids and their (y, z) dimensions are indicated in Fig. 2c. The x dimensions of the $1/e^2$ and 1/e ellipsoids (not shown in Fig. 2c) are $\Delta x(1/e^2) = 2b_o$ and $\Delta x(1/e) = \sqrt{2}\, b_o$, respectively. Note that the $1/e^2$ ellipsoid passes through the intersection of the $1/e^2$ intensity profiles of the two beams, whereas the 1/e ellipsoid is tangent to the $1/e^2$ intensity profiles. The latter is evident because the signal current (excursion) amplitude varies in proportion to $\sqrt{S_1 S_2}$ where S_1 and S_2 are the local intensities of the two illuminating beams. It should be noted that these relative signal amplitude ellipsoids are identical to those of a cross-beam, reference beam velocimeter (Ref. 7), and thus the dual-scatter technique provides spatial resolution identical to that of a practical reference beam velocimeter.

The $1/e^2 = 0.135$ relative signal amplitude ellipsoid will be chosen to define the probe volume of the detection system. Thus the $1/e^2$ ellipsoid probe volume encompasses all space within which the relative Doppler signal (excursion) amplitude is at least $1/e^2 = 0.135$ of the peak signal amplitude existing at the geometrical center of the probe volume (0, 0, 0). The volume of the $1/e^2$ ellipsoidal probe volume is

$$V = \frac{\pi}{3} \frac{(2b_o)^3}{\sin\theta} = \frac{8}{3\pi^2 \sin\theta} \left(\frac{f_L \lambda}{b}\right)^3 \cong \frac{8 f_L{}^4 \lambda^3}{3\pi^2 D b^3} \tag{7}$$

where Eq. (3) was first substituted for b_o and the approximation $\sin \theta \approx (D/f_L)$ (see Fig. 1) was then employed. The variables of Eq. (7) are shown in Figs. 1 and 2.

The $1/e^2$ probe volume can be made as small as 5×10^{-10} cm^3 (for $f_L/b = 20$, $\theta = 30$ deg, and $\lambda = 4.88 \times 10^{-5}$ cm) with a practical self-aligning optical system.

Note for small θ such that $\sin \theta \approx \theta$ (radians) and $\cos \theta \approx 1$, the probe volume ellipsoid is of circular (x, y) cross section. Thus, a diameter and length dimension sufficiently describe the probe volume.

3.1 PROBE VOLUME MEASUREMENT

Figures 4, 5a, and 5b present data that experimentally verify that probe volume dimensions can be achieved which are very close to the theoretical limit. Figures 4 and 5a contain oscilloscope displays of the real-time Doppler signals caused by a small (approximately 5-μm) wire passing through the probe volume at a constant velocity of 15.7 in./sec. The wire was carefully positioned such that its length dimension was parallel to the fringes (parallel to the x axis of Fig. 2) and such that the wire velocity was orthogonal to the fringes and parallel to the y axis of Figs. 1 and 2. The trace of Fig. 4 was caused by a wire trajectory approximately through the center of the probe volume such that it crossed the z axis at $z \approx 0$. For the experimental parameters of Fig. 4, the $1/e^2$ ellipsoidal probe volume diameter has a theoretical (Eqs. (3) and (4)) diameter of $\Delta x(1/e^2) \approx \Delta y(1/e^2) = 0.022$ in. This agrees very closely with the experimentally determined value (Fig. 4) of $\Delta y(1/e^2) = 0.021$ in.

The length $\Delta z(1/e^2)$ of the probe volume was obtained using the data of Fig. 5a, which is plotted in Fig. 5b. The data of Fig. 5a were recorded (with parameters identical to those of Fig. 4) by successively increasing the z position of the traversing wire by 0.1 in., where z' (Fig. 5) $\approx$ z (Figs. 1 and 2) + 0.48 in., such that the geometrical center of the probe volume was located at $z' \approx 0.48$ in. The data were restricted because of the limited z traverse capability of the micrometer traverse table used. For the data of Figs. 5a and b, the theoretically and experimentally determined probe volume length dimensions were $\Delta z(1/e^2) =$ 0.956 and 1.00 in., respectively, which again agree very well.

3.2 NUMBER OF CYCLES OF FREQUENCY INFORMATION

A knowledge of the fringe spacing (Eq. (1)) and the dimensions of the $1/e^2$ relative signal amplitude ellipsoid (Fig. 2c and Eq. (4)) allows one to predict the number of cycles of frequency information, N, generated by a scatter center passing through the center of the probe volume along the y axis

$$N(1/e^2) = 2b_o \, 2 \tan(\theta/2)/\lambda = \frac{4}{\pi} \frac{D}{2b} \tag{8}$$

where N is the number of cycles between $1/e^2$ relative signal amplitude points, $D = 2f_L \tan \theta/2$ (Fig. 1a) is the beam spacing ahead of the lens, 2b is the beam diameter ahead of the lens, and Eq. (3) has been substituted for $2b_o$. Thus, the maximum number of cycles is independent of f_L, the focal length of the beam focusing lens, and is determined solely by the ratio of the input beam spacing to the input beam diameter, D/2b.

Modifying the illuminating optics to provide a reduced number of cycles, N, will obviously reduce the velocity measurement accuracy. Also, as the velocity vector is rotated from orthogonal to the fringes (parallel to the y axis) to an orientation parallel to the fringes (parallel to the y = 0 plane), the number of cycles N will obviously approach zero, as in the limiting case, the scatter center trajectory will be parallel to the fringes and zero cycles of frequency information must result. The latter problem is not peculiar to the dual-scatter LDV, as any heterodyning LDV has both a characteristic probe volume of finite (x, y, z) dimensions and an equivalent set of probe volume fringes which cause the device to be velocity component selective. Thus, the accuracy of the dual-scatter LDV is seen to be dependent upon the orientation of the velocity vector relative to the probe volume fringes, and such a limitation is common to all heterodyning LDVs.

The experimental data of Figs. 4 and 5 indicate that the experimentally and theoretically determined maximum number of cycles agree quite well. A sample calculation of N is shown in Fig. 4.

SECTION IV
SIGNAL-TO-NOISE PERFORMANCE

4.1 EFFECT OF SCATTERING DIRECTION

The chief advantage of the dual-scatter LDV, in comparison to reference beam heterodyning LDVs, is derived from the fact that the

detected frequency is independent of the scattering direction. This permits very large solid angles of scattered light to be collected, thereby providing enhanced signal-to-noise (S/N) performance. With conventional reference beam heterodyning LDVs, the collection and alignment of scattered light must be severely restricted to limit the signal frequency broadening effects (Refs. 1, 2, and 7).

Figure 6 presents experimental data which demonstrate that, with relatively light seeding conditions, the S/N performance of a dual-scatter LDV is superior to that of a reference beam LDV employing similar laser power. Both sets of data were recorded using similar self-aligning optical systems operating in a small angle front-scatter mode. The reference beam data were high-pass filtered before being displayed, but the dual-scatter were not. The seed density (smoke generator output) was adjusted to provide just enough seeding to produce a continuous signal. Both spectrum analyzer traces were recorded on a Tektronix IL20 spectrum analyzer set on "linear" vertical display. Both signals were attenuated at various levels to provide presentable displays. The frequency spread of the dual-scatter spectrum analyzed signal is attributable to the finite number of cycles generated by scatterers passing through the probe volume.

The comparative signal-to-noise performance is evident in the spectrum analyzer displays. The difference between the base line trace, recorded with 40-db signal attenuation, and the minimum attainable level outside of the signal frequency domain is representative of the shot noise caused by the net detector input radiation power. This noise level is unmeasurably low for the dual-scatter LDV, but it comprises a level of about 5 percent of the peak spectral content of the reference beam system.

4.2 EFFECT OF SEED DENSITY

As the smoke generator output was increased, both signal amplitudes increased. The reference beam noise level did not increase, however, because this noise is determined primarily by the constant input power of the reference beam (see Ref. 7, for example). Thus the, attenuated, spectrum analyzed S/N performance of the reference beam LDV increased to an unmeasurably high level similar to that of the initial dual-scatter spectrum analyzed display. The dual-scatter noise level, however, increased at a much faster rate than did its peak (spectrum analyzed) signal amplitude, such that its (attenuated) spectrum analyzed S/N performance decreased to a level comparable to that of the initial reference beam spectrum analyzed display. The dual-scatter S/N decreased because:

1. The in-phase signals generated by many scatter centers will add only if adjacent scatterers are separated by a y distance of one fringe spacing, $\Delta y = (\lambda/2)/\sin(\theta/2)$. If, for example, two scatterers are separated by a y distance of $\Delta y/2$, the two signals will be 180 deg out of phase and will cancel one another. The cross-heterodyne signals will mostly be negligible, for large solid angle scattered collection, because two radiations scattered from different particles will generally not be aligned to within a fraction of a wavelength over the collection aperture (Ref. 7). A more qualitative analysis will reveal that ten identical, randomly located scatterers will generate 2.3 times as much signal amplitude as one scatterer, 100 scatterers will generate 7.2 times that of 1, 1000 scatters will generate 23 times that of 1, and so on.
2. The net photodetector direct current and the shot noise power will (for random particle locations) increase in direct proportion to the number of scatter centers in the probe volume. Thus m scatterers will generate m times as much direct current and shot noise power.

For these reasons the dual-scatter signal-to-noise ratio decreases with increasing seed density and this system is ideally suited for low seed conditions. With reference beam LDV systems, the signal amplitude increases for reasons similar to (1) above, where cross-heterodyne current contributions are now negligible because of the dominance of the reference beam power at the photodetector, the increased detector radiation power attributable to many scatterers being negligibly small. Thus the reference beam LDV is ideally suited for high seed conditions, although for low velocity, real-time single particle frequency bursts have been observed with a 20-mw reference beam system scattering from atmospheric impurities.

SECTION V
DUAL-SCATTER, BACK-SCATTER LDV

A dual-scatter, back-scatter LDV used at the AEDC is shown in Fig. 7. The back-scattered radiation, dashed, is collimated by lens L1 and passes over the thin (x-dimension) blocks B1 and B2 before being collected (L2), spatially filtered (PH), and detected (PT). This system design is advantageous because:

1. The optics, with exception of the focusing lens (L1), can be mounted to a small mechanical reference frame such that once adjusted to image the probe region P onto pinhole PH, the system performance will be insensitive to mechanical vibrations and movement of the focusing lens L1.

2. The lens L1 can then be traversed along its axis to vary the location of the probe volume P. The signal strength will not deteriorate because of small off-axis displacements or rotations of lens L1.

3. The probe volume may easily be traversed by adding a mirror arrangement between lens L1 and lens L2, thereby allowing independent motion of lens L1 with respect to the remaining hardware of the velocimeter. It is shown in Fig. 7 that only lens L1 determines the location of the probe volume P, thereby producing a one-to-one correspondence between lens L1 and probe volume motion. None, one, or more of these mirrors can then be translated with lens L1 to move the measurement point P in one, two, or three orthogonal directions. The received signal will not deteriorate because of such translations, thus permitting the probe volume to be traversed throughout the test region.

4. Beam expansion and refocusing optics can be used in place of lens L1 to provide a more efficient system with a smaller probe volume than would otherwise be attainable at a large measuring distance (distance from compound L1 element to P). The probe volume of this system also can be translated, via mirrors, in three orthogonal directions.

5. The system is readily adaptable to the measurement of two orthogonal velocity components by employing different blocks, other than B1 and B2, that cause three parallel illuminating beams to exit from the stationary package (onto L1). All of the previously mentioned advantages would apply also to the two-component system.

6. The third orthogonal velocity component could be added by splitting off a small portion of the laser power and heterodyning it with backscattered radiation. All of the previously mentioned advantages would apply also to this three-component system.

SECTION VI
CONCLUSIONS

The performance of a new, focused, crossed-beam, dual-scatter, laser velocity meter (anemometer) was described as resulting from the establishment of stationary interference fringes (Eqs. (1) and (2), Figs. 1 and 2). Velocity information is obtained by recording the signal frequency of detected radiation scattered from impurity particles passing through the fringes of the beam crossover region. The frequency to velocity conversion (Eq. (2)) is identical to that of a crossed-beam reference beam LDV system, and the system is sensitive to only that velocity component orthogonal to the fringes. The system spatial resolution is identical to that of a crossed-beam, reference beam LDV (Eqs. (3) through (7) and Figs. 2 through 5). The chief advantage of the system (in comparison to front scatter reference beam LDVs) is that larger quantities of scattered radiation can be collected, thereby providing increased sensitivity and a system potentially capable of measuring very high velocity or low seed density fluid flows. A dual-scatter, back-scatter LDV unit was described.

REFERENCES

1. Lennert, A. E., Brayton, D. B., Crosswy, F. L., Goethert, W. H., and Smith, F. H. "Summary Report of the Development of a Laser Velocimeter to be used in AEDC Wind Tunnels." AEDC-TR-70-101, July 1970.

2. Angus, J. C., Morrow, D. L., Dunning, J. W., and French, M. J. Motion Measurements by Laser Doppler Techniques. Industrial and Engineering Chemistry, Vol. 61, No. 2, February 1969. (This paper contains many additional references.)

3. Bourquin, K. R. and Shigemoto, F. H. "Investigation of Air-Flow Velocity by Laser Backscatter." NASA TN D-4453, April 1968.

4. Penny, C. M. "Differential Doppler Velocity Measurements." IEEE Journal of Quantum Electronics, June 1969.

5. Mayo, W. T., Jr. Simplified Laser Doppler Velocimeter Optics. To be published.

6. Mazumder, M. K. and Wankum, D. L. "SNR and Spectral Broadening in Turbulence Structure Measurement Using CW Laser." IEEE Journal of Quantum Electronics, June 1969.

7. Brayton, D. B. "A Simple Laser, Doppler Shift, Velocity Meter with Self-Aligning Optics." Proceedings, Electro-Optical Systems Design Conference, New York, N. Y., September 1969.

8. Kogelnik, H. "Imaging of Optical Modes - Resonators with Internal Lenses." The Bell System Technical Journal, March 1965.

APPENDIX
ILLUSTRATIONS

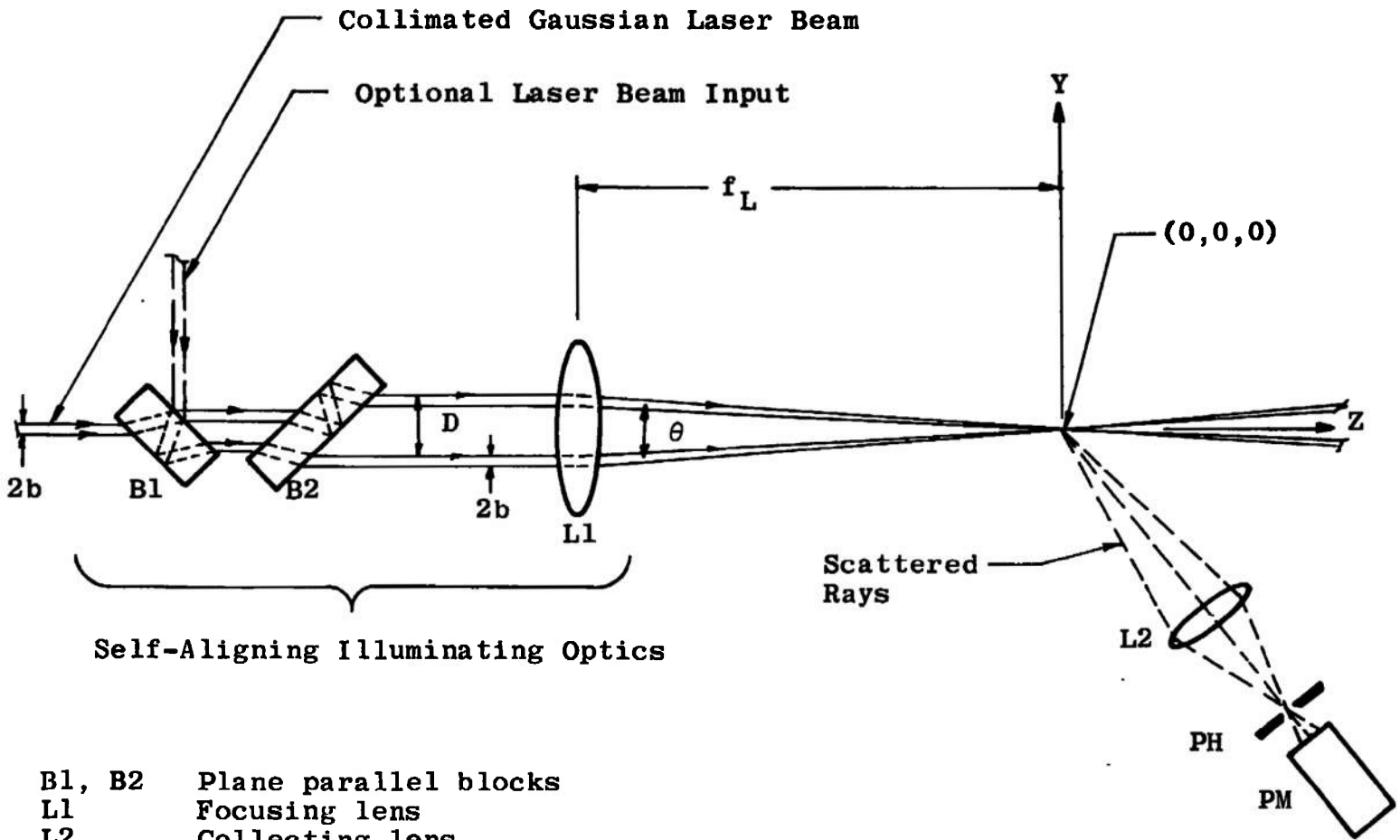

B1, B2	Plane parallel blocks
L1	Focusing lens
L2	Collecting lens
(0,0,0)	Beam crossover region
PH	Pinhole
PM	Photomultiplier tube

a. Schematic of Optical Arrangement

Fig. 1 Self-Aligning Dual-Scatter Optics

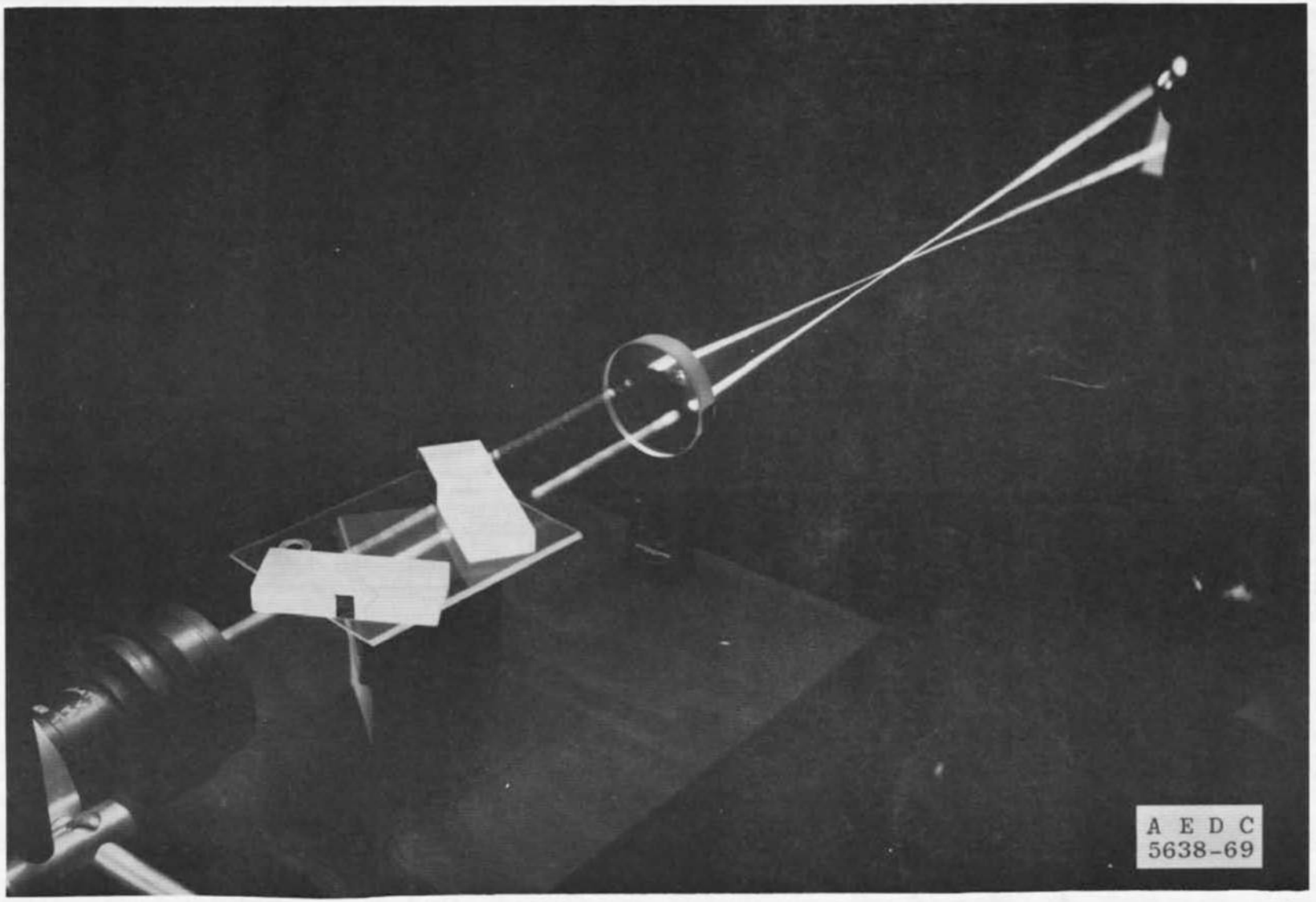

b. Photograph of Self-Aligning Optics Illuminated by a Laser

Fig. 1 Concluded

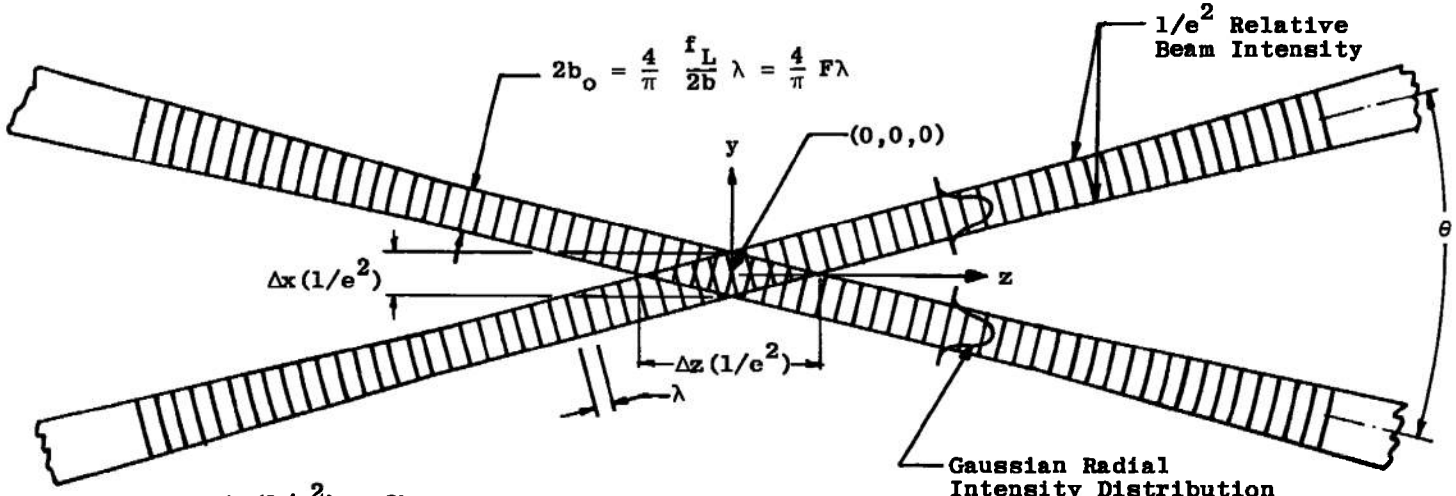

a. Schematic of Beam Crossover Region

Fig. 2 Laser Beam Crossover Region

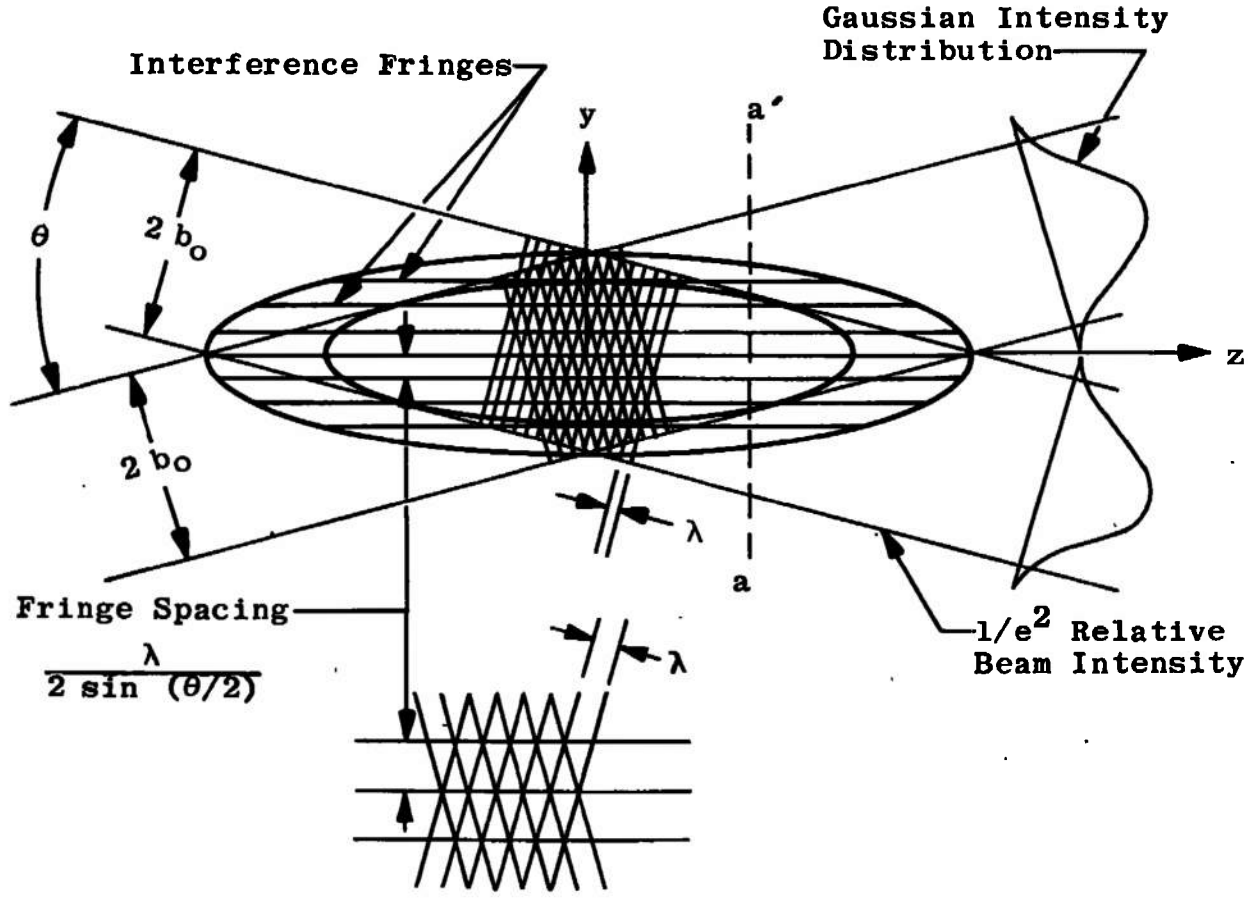

b. Beam Crossover Fringes

Fig. 2 Continued

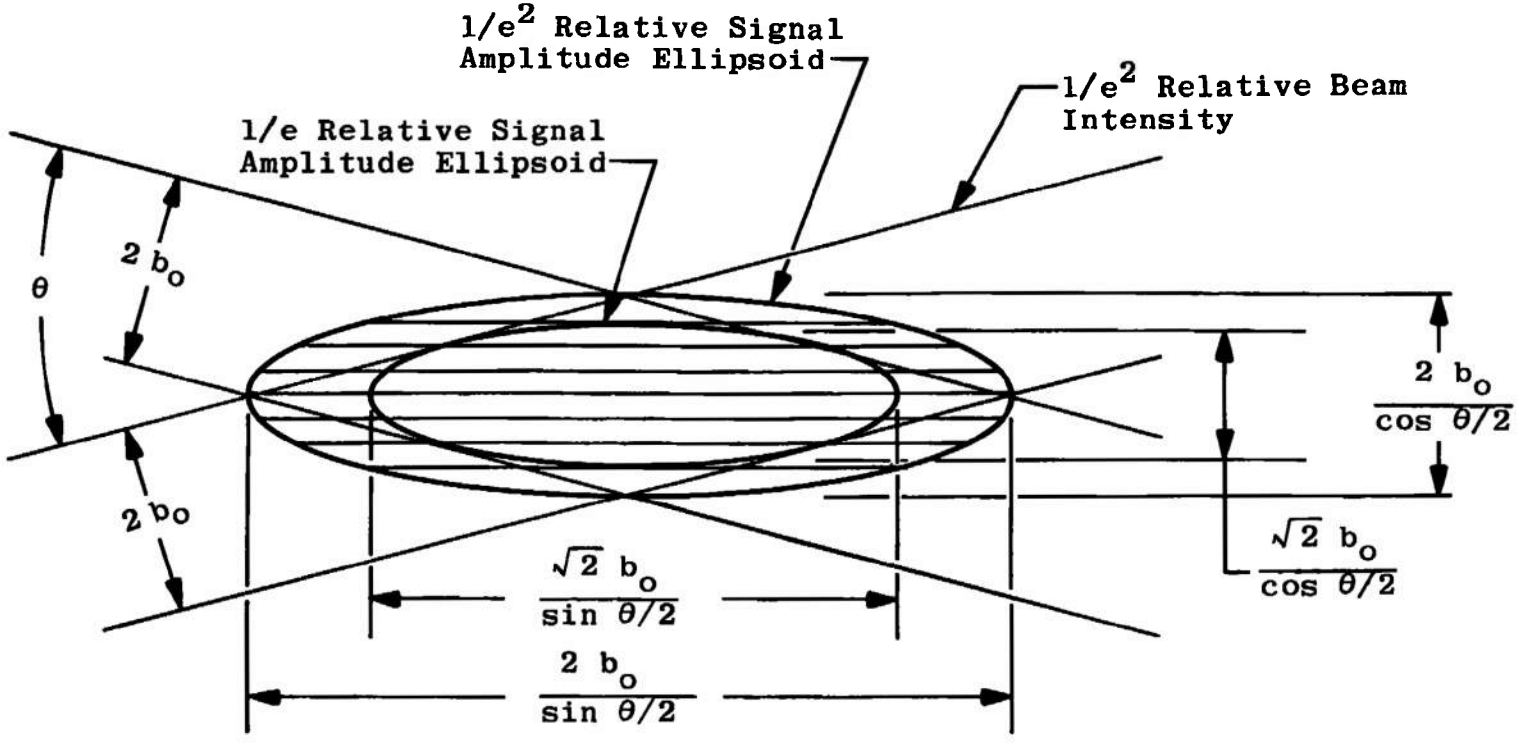

c. Relative Signal Amplitude Ellipsoids

Fig. 2 Concluded

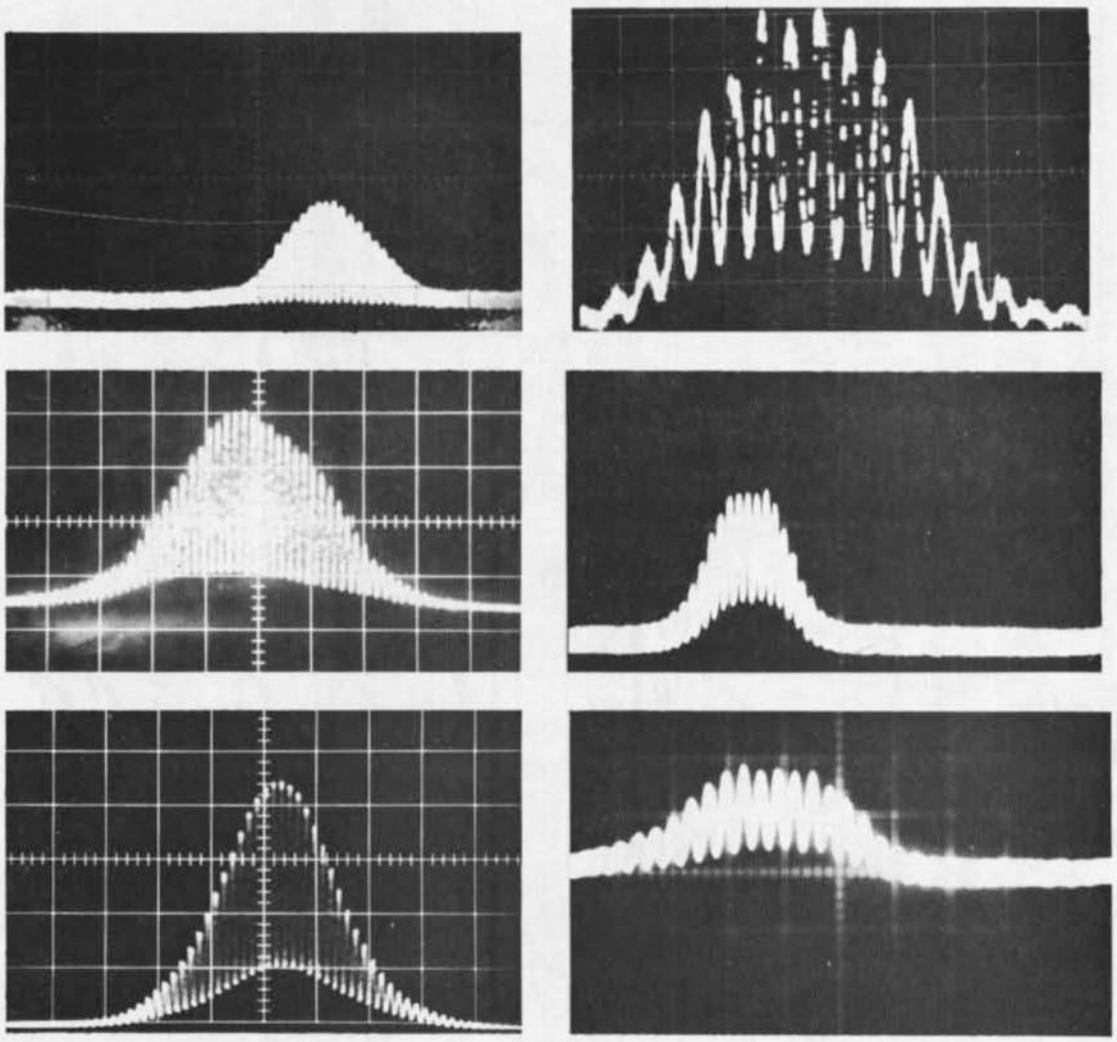

a. Particles Traversing Near Y Axis, Displaying Scattered Intensity versus Position Parallel to Y Axis

Fig. 3 Real-Time Display of Particles Traversing Probe Volume

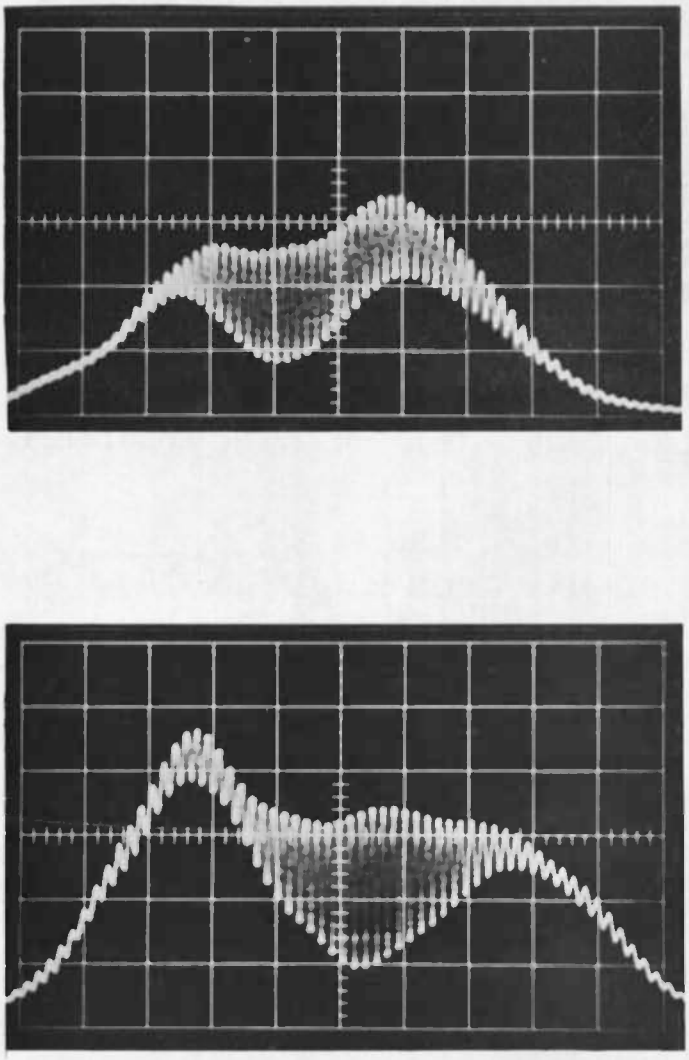

b. Particles Traversing Off Y-Axis
Fig. 3 Concluded

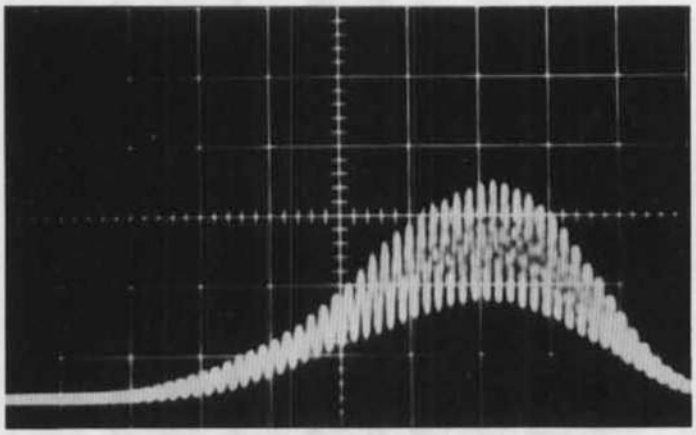

Parameters: λ - 6328 Å

2b - 0.11 cm (S.P. Model 124 laser)

f_L - 30 in.

D - 1.30 in.

Horiz. Display - 0.2×10^{-3} sec/cm

Theoretical: $\Delta y\ (1/e^2) = \frac{4}{\pi} \frac{f_c}{25} \frac{\lambda}{\cos \theta/2} = 0.022$ in.

$$N = \frac{4}{\pi} \frac{D}{2b} = 38.2 \text{ cycles}$$

Experimental: Wire velocity - 15.7 $\frac{\text{in.}}{\text{sec}}$

$\Delta y\ (1/e^2)$ = (Scope Sweep Speed)
($1/e^2$ Distance from Photograph above)
(Wire Velocity)

$$\Delta y\,(1/e^2) = \left(0.2 \times 10^{-3} \frac{\text{sec}}{\text{cm}}\right) (6.6 \text{ cm}) \left(15.7 \frac{\text{in.}}{\text{sec}}\right) = 0.021 \text{ in.}$$

N = 37 cycles Counted from Photograph above

Fig. 4 Comparison between Theoretical and Experimental Probe Volume Diameter

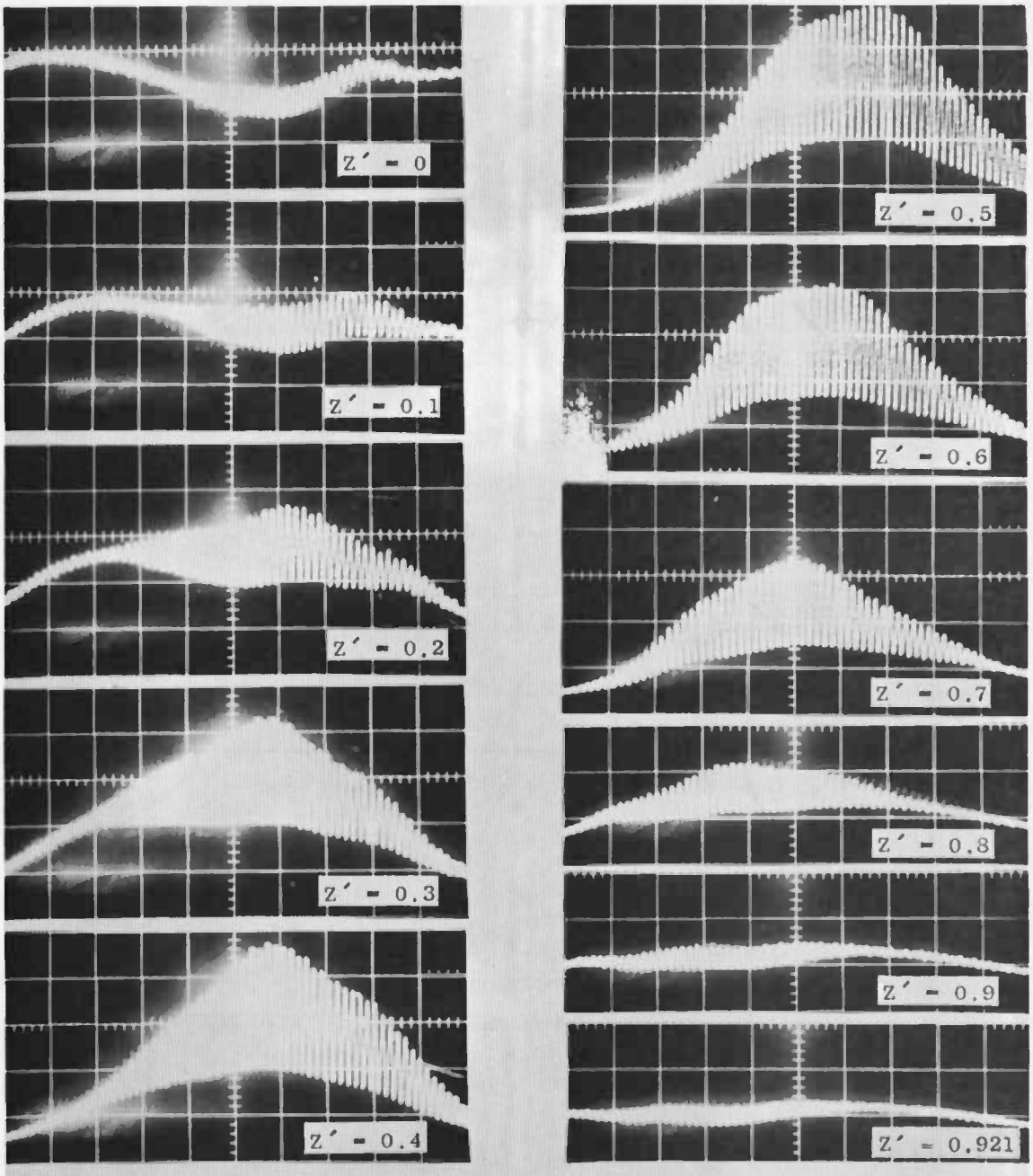

a. Real-Time Display of Z-Axis Doto Points, Showing Scattering Intensity versus Position along Y Axis

Fig. 5 Experimental Dota for Determinotion of Probe Volume Length

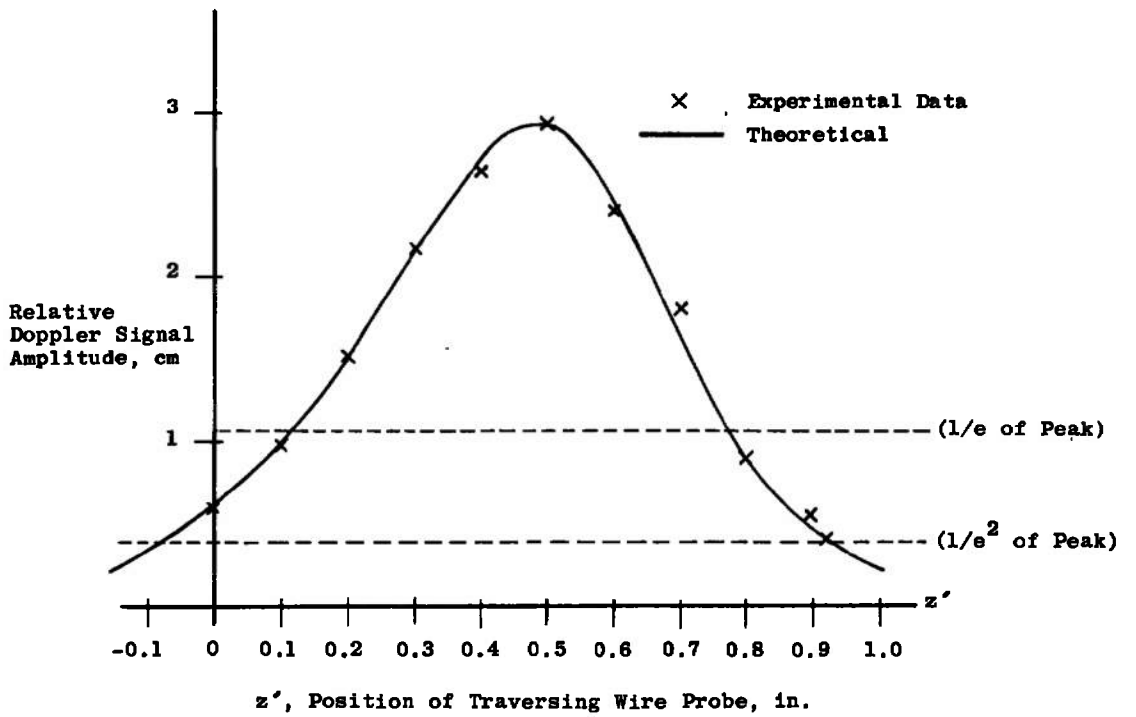

Experimental:

$\Delta z(1/e) = 0.785 - 0.135 = 0.650$ in.

$\Delta z(1/e^2) = 0.930 + 0.07 = 1.00$ in.

Theoretical: (LDV Parameters Same as Those of Fig. 4):

$\Delta z(1/e) = \sqrt{2} b_o / \sin(\theta/2) = 0.676$

$\Delta z(1/e^2) = 2b_o / \sin(\theta/2) = 0.956$

b. Plot of Data of Fig. 5a (Comparison between Theoretical and Experimental Probe Volume Length)

Fig. 5 Concluded

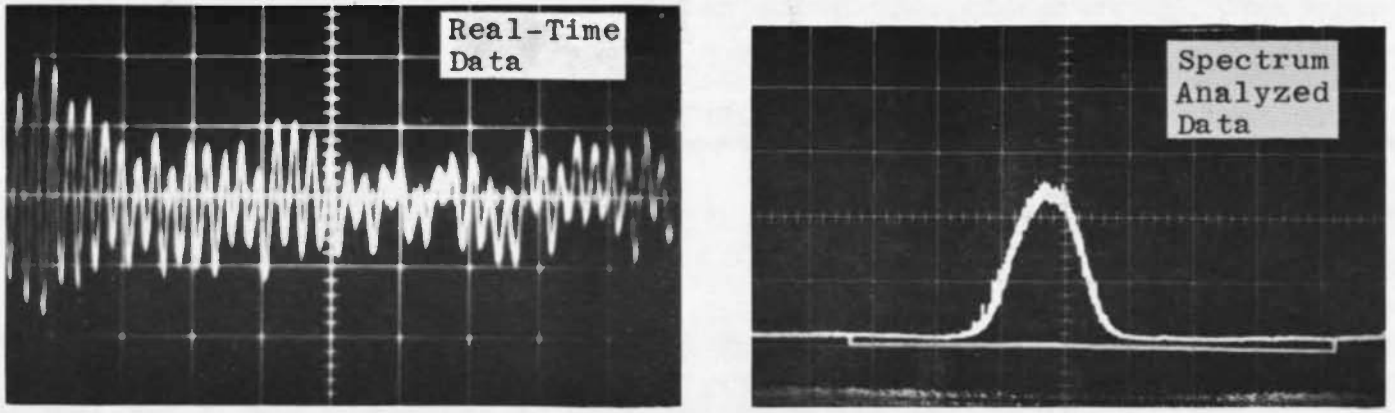

a. Reference Beam LDV Data

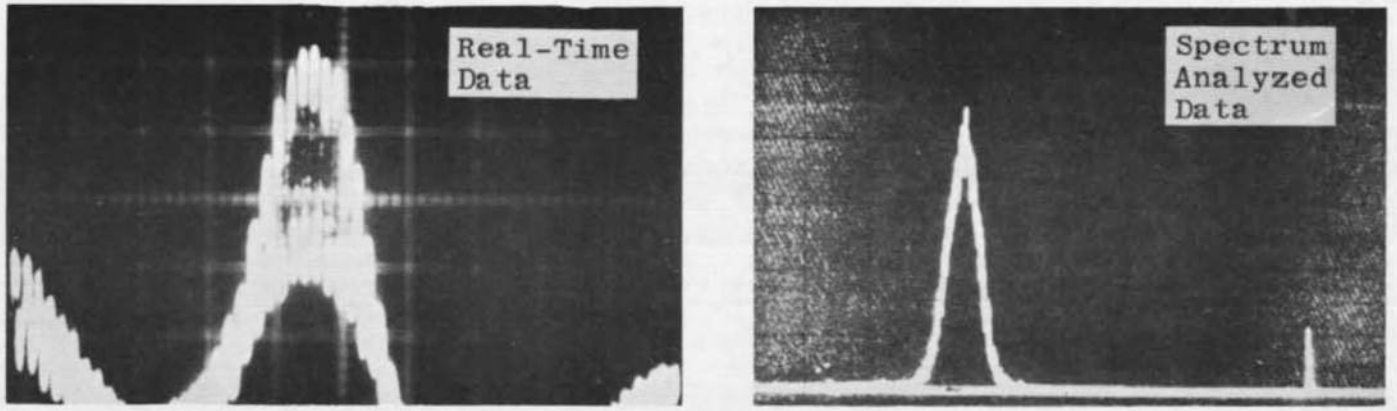

b. Dual-Scatter LDV Data

Fig. 6 Comparison of Reference Beam LDV and Dual-Scatter LDV Data

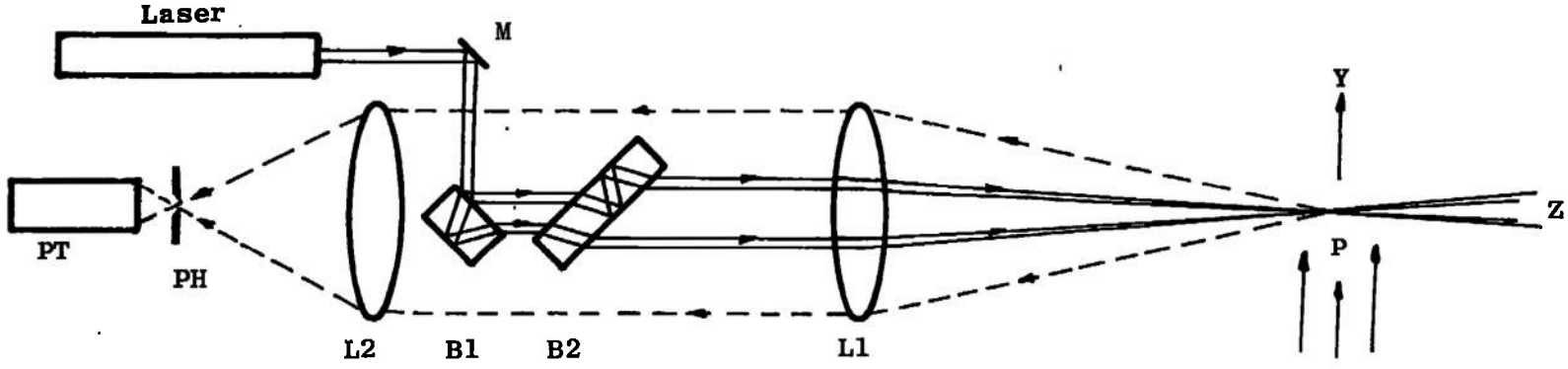

B - Plane Parallel Block
L - Lens
M - Mirror
P - Probe Volume
PH - Pinhole
PT - Photomultiplier Tube

Fig. 7 Dual-Scatter, Back-Scatter LDV Optical Arrangement

UNCLASSIFIED

Security Classification

DOCUMENT CONTROL DATA - R & D

(Security classification of title, body of abstract and indexing annotation must be entered when the overall report is classified)

1. ORIGINATING ACTIVITY *(Corporate author)*
Arnold Engineering Development Center
ARO, Inc., Operating Contractor
Arnold Air Force Station, Tennessee

2a. REPORT SECURITY CLASSIFICATION
UNCLASSIFIED

2b. GROUP
N/A

3. REPORT TITLE

NEW VELOCITY MEASURING TECHNIQUE USING DUAL-SCATTER LASER DOPPLER SHIFT

4. DESCRIPTIVE NOTES *(Type of report and inclusive dates)*
Final Report July 1969 to July 1970

5. AUTHOR(S) *(First name, middle initial, last name)*

D. B. Brayton and W. H. Goethert, ARO, Inc.

6. REPORT DATE	7a. TOTAL NO. OF PAGES	7b. NO. OF REFS
November 1970	33	8

8a. CONTRACT OR GRANT NO.
F40600-71-C-0002

b. PROJECT NO.
4344

c.
Program Element 65701F

d. Task 32

9a. ORIGINATOR'S REPORT NUMBER(S)
AEDC-TR-70-205

9b. OTHER REPORT NO(S) *(Any other numbers that may be assigned this report)*
ARO-OMD-TR-70-199

10. DISTRIBUTION STATEMENT This document is subject to special export controls and each transmittal to foreign governments or foreign nationals may be made only with prior approval of Arnold Engineering Development Center (XON), Arnold Air Force Station, Tennessee 37389.

11. SUPPLEMENTARY NOTES
Available in DDC

12. SPONSORING MILITARY ACTIVITY
Arnold Engineering Development Center, AFSC, Arnold Air Force Station, Tennessee 37389

13. ABSTRACT

Conventional laser Doppler velocimeters (LDV) detect velocity by heterodyning scattered, Doppler shifted radiation with unscattered, reference radiation. A new dual-scatter LDV technique is described which simultaneously illuminates a moving scatterer from two different directions and heterodynes the two superimposed radiations simultaneously scattered in a common direction. Significant advantages are derived from the fact that the Doppler difference frequency thus obtained is independent of the scattered direction, permitting unusually large quantities of scattering radiation to be collected without adversely affecting the signal frequency dispersion; these advantages include enhanced signal-to-noise performance and a capability to measure fluid flows with unusually high velocity and/or low seed density. System performance, experimental verifications, and typical system designs are presented.

This document has been approved for public release and sale; its distribution is unlimited. Per A F Letter dtd 9 July 1974 Signed William O. Cole.

DD FORM 1 NOV 68 1473

UNCLASSIFIED

Security Classification

14. KEY WORDS	LINK A		LINK B		LINK C	
	ROLE	WT	ROLE	WT	ROLE	WT
1 anemometers						
speed indicators						
2 lasers						
3 doppler effect						
wind tunnels						
fluid flow - gases						
4. Velocimeters						
5. Flow -- Measurement by						
5. Laser doppler velocimeters						

AFSC
Arnold AFS Tenn